A Journal of the Gesellschaft Deutscher Chemiker

Angewandte Chemie

GDCh

International Edition

www.angewandte.org

Accepted Article

Title: Tetra-benzothiadiazole-based [12]Cycloparaphenylene with Bright Emission and its Supramolecular Assembly

Authors: Zhen-Lin Qiu, Chun Tang, Xin-Rong Wang, Yang-Yang Ju, Ke-Shan Chu, Ze-Ying Deng, Hao Hou, Yu-Min Liu, and Yuan-Zhi Tan

To be cited as: *Angew. Chem. Int. Ed.* 10.1002/anie.202008505

Link to VoR: https://doi.org/10.1002/anie.202008505

WILEY-VCH

Angewandte Chemie International Edition 10.1002/anie.202008505

Tetra-benzothiadiazole-based [12]Cycloparaphenylene with Bright Emission and its Supramolecular Assembly

Zhen-Lin Qiu,[a] Chun Tang,[a] Xin-Rong Wang,[a] Yang-Yang Ju,[a] Ke-Shan Chu,[a] Ze-Ying Deng,[a] Hao Hou,[a] Yu-Min Liu, [a] Yuan-Zhi Tan*[a]

Abstract: The radial conjugated π-system of cycloparaphenylenes (CPPs) makes them as intriguing fluorophores and unique supramolecular host, however, the bright photoluminescence (PL) of CPPs was limited to the blue light and the supramolecular assembly behavior of large CPPs was rarely investigated. Here we present the synthesis of tetra-benzothiadiazole-based [12]cycloparaphenylene (TB[12]CPP), which exhibits a lime to orange PL with an excellent quantum yield up to 82%. The PL quantum yield of TB[12]CPP can be further improved to 98% in polymer matrix. Benefiting from its enlarged size, TB[12]CPP can accommodate a fullerene derivative or concave-convex complexes of fullerene and buckybowl through the combined π–π and C-H···π interactions. The latter one demonstrates the first case of ternary supramolecule of CPPs.

Cycloparaphenylenes (CPPs), composed of *para*-linked phenylene, are regarded as the shortest segment of carbon nanotube (CNT) and thus also referred as carbon nanohoops[1]. As the segment of CNT, CPPs were used as the seed molecules for the growth of well-defined single wall CNTs[2]. Different from the cyclic-*meta*-phenylenes and cyclic-*ortho*-phenylenes[3], the synthesis of CPPs was achieved until last decade[4], that is likely attributed to the larger ring strain of CPPs. The cyclic conjugated π-system of CPPs renders them unique electronic and optical properties[5]. For instance, most of CPPs present highly emissive behavior with high quantum yield and large Stokes-shift[6]. In addition, the macrocyclic structure of CPPs hinders the intermolecular π–π stacking, consequentially makes CPPs more soluble in different solvents than their linear counterparts[7], leading to a good solvent tolerance of their photoluminescence (PL). However, the CPPs with high PL quantum yield (PLQY) only emit blue light[5]. Although the red-shifted PL up to 500 nm can be realized by decreasing the size of CPPs[8] or incorporation of donor-acceptor structure[9], these strategies to red-shift PL of CPPs resulted in a dramatic decrease of PLQY.

On the other hand, the shape-persistent macrocyclic structure of CPPs provides inner cavity for supramolecular assembly[10], which has attracted increasing interests. The radially-oriented π-system of CPPs enables effective π–π interactions with spherical fullerenes[11]. The first reported CPP supramolecule is C_{60}@[10]CPP, which is regarded as the shortest CNT peapod[11a]. Moreover, the assembly of carbon nanohoops with planar or curved polyaromatic hydrocarbons (PAHs) based on C-H···π interactions was achieved[12], as a complement to the π–π complex. Among them, the ring size plays an important role in the supramolecular assembly of CPPs. For instance, the CPPs smaller than [10]CPP only show ability to accommodate solvent molecules. On the contrary, the enlarged inner space of large CPPs, such as [12]CPP, provides the additional opportunities to accommodate larger and more complex guests other than bare fullerenes.

Here we show the synthesis of tetra-benzothiadiazole-based [12]cycloparaphenylene (TB[12]CPP) by a platinum-mediated cyclization[8a, 13]. The structure of TB[12]CPP was unambiguously identified by mass spectroscopy, NMR and single crystal X-ray diffraction (SCXRD). Introducing benzothiadiazole units red-shifts the UV-Vis absorption and PL of TB[12]CPP by 89 nm and 119 nm, respectively, compared with the pristine [12]CPP. TB[12]CPP shows a high PLQY up to 82%. In polymer matrix, its PLQY can be improved to nearly 100%. Taking advantage of the enlarged size of TB[12]CPP, TB[12]CPP can assemble with a Diels-Alder adduct of C_{60} and anthracene (anthracene-C_{60}) by both π–π and C-H···π interactions. More importantly, the ternary complexes of CPPs are achieved for the first time by hosting the concave-convex supramolecule of fullerene (C_{60} or C_{70}) and buckybowl (trithiasumanene) in the inner cavity of TB[12]CPP.

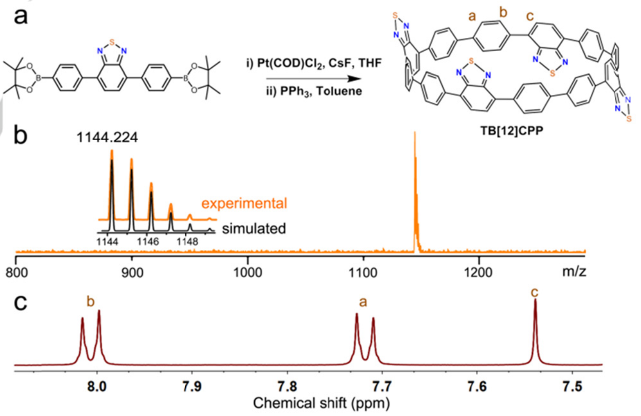

Figure 1. Synthesis of TB[12]CPP. (a) synthetic route of TB[12]CPP. (b) The mass spectra of TB[12]CPP. The isotopic distribution for the mass peak of TB[12]CPP is shown as the insert figure. (c) ^{1}H NMR spectrum of TB[12]CPP measured in $CDCl_3$.

The bottom-up organic synthesis of CPPs facilitates the incorporation of chromophores into the scaffold of CPPs. Benzothiadiazole is the widely used building unit to red-shift the optical absorption and PL of the conjugated polymers[14]. Thereby, the incorporation of benzothiadiazole units can impart CPPs with enhanced emission performance, which was also demonstrated in the Jasti's recent work[15]. Accordingly, a rational repeating unit 4,7-diphenyl-benzothiadiazole was designed to construct TB[12]CPP, in which the platinum-

---

[a] Z. L. Qiu, C. Tang, X. R. Wang, Y. Y. Ju, K. S. Chu, Z. Y. Deng, H. Hou, Dr. Y.M. Liu, Prof. Dr. Y. Z. Tan
State Key Laboratory for Physical Chemistry of Solid Surfaces, Collaborative Innovation Center of Chemistry for Energy Materials, and Department of Chemistry, College of Chemistry and Chemical Engineering, Xiamen University, Xiamen 361005, China
E-mail: yuanzhi_tan@xmu.edu.cn

Supporting information for this article is given via a link at the end of the document.

10.1002/anie.202008505

mediated assembly method was used for the cyclization[8a, 13]. Frist, the *para*-borylated 4,7-diphenyl-benzothiadiazole was synthesized by Miyaura borylation of 4,7-bis(4-bromophenyl)-benzothiadiazole. Then, the *para*-borylated 4,7-diphenyl-benzothiadiazole was reacted with Pt(COD)Cl_2 in dry THF under reflux for 24 h. Then the resultant mixture was subjected to reductive elimination in toluene at 110 °C for 48 h in presence of triphenylphosphine (Figure 1a). After reaction, the crude products were extracted by dichloromethane and separated by silica gel column chromatography to obtain TB[12]CPP (10% over two steps) (Supporting Information S2 and Figures S1-S5). The high-resolution MALDI-TOF mass spectrum of TB[12]CPP ($C_{72}N_8S_4H_{40}$) showed an experimental molecular weight of 1144.224 Da (calculated 1144.225 Da) (Figure 1b). The ^{1}H NMR spectrum of TB[12]CPP shows two double and one singlet signals (Figure 1c). Both the mass spectrometry and NMR analysis (Figure 1 and Figures S3-S5) confirm the successful synthesis of TB[12]CPP.

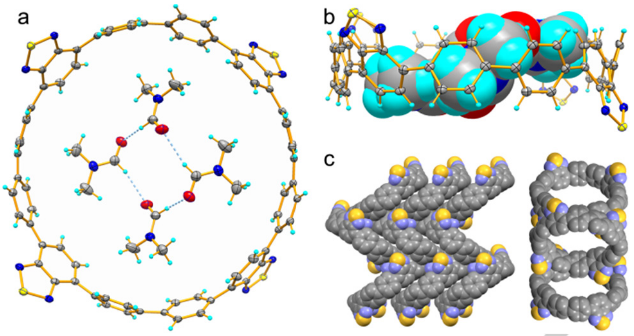

Figure 2. Crystal structure of TB[12]CPP. (a. b.) Top and side views. Thermal ellipsoids were set at 50% probability level. The inner DMF molecules in the side view was represented in spacefill model for clarity. The non-conventional hydrogen bonds were shown as sky blue dashed lines. (c) The packing structure of TB[12]CPP in solid state. The hydrogen atoms and DMF molecules were omitted in packing structure.

The structure of TB[12]CPP was further revealed by SCXRD (Figure 2). The crystals of TB[12]CPP were grown by slow evaporation of its *N*,*N*-dimethylformamide (DMF) solution. In the crystalline state, TB[12]CPP adopts a conformation with two adjacent benzothiadiazole units above and the other two below the plane of the inner cycle (Figure 2b). The small variation between the shortest and longest distances through the ring centroid (16.2–16.8 Å, Figure 4g) indicates the high circularity of TB[12]CPP. Interestingly, four ordered DMF molecules are hosted inside the TB[12]CPP (Figures 2a and 2b), forming a supramolecular tetramer by non-conventional hydrogen bonds[16] (Figure 2a), which indicates the possibility of supramolecular assembly inside CPP rings. Similarly with [12]CPP,[17] TB[12]CPP packs into a tubular structure (Figure 2c). Between the tubular supramolecular structures, TB[12]CPP aligns in a herringbone manner (Figure 2c).

TB[12]CPP is well soluble in common organic solvents, such as toluene, chloroform, THF and DMF. Different from the nearly colorless solution of [12]CPP, the solution of TB[12]CPP is yellow, indicating an obvious red-shift of its absorption. The UV-Vis spectrum of TB[12]CPP measured in chloroform, shows two major absorption bands at 320 and 428 nm, which is red-shifted by 89 nm and 27 nm with respect to that of [12]CPP[18] and 4,7-diphenyl-benzothiadiazole (Figure S6), respectively. The extinction coefficient of TB[12]CPP was measured to be 8.3×10^4 $M^{-1}cm^{-1}$ at 318 nm and 6.4×10^4 $M^{-1}cm^{-1}$ at 427 nm, comparable with that of [12]CPP (1.4×10^5 $M^{-1}cm^{-1}$),[18] but an order of magnitude higher than that of 4,7-diphenyl-benzothiadiazole (6.8×10^3 $M^{-1}cm^{-1}$ at 401 nm). According to the time-dependent density functional theory (TD-DFT) calculations (Supporting Information S3 and Figures S9-S10), the absorption band at 428 nm of TB[12]CPP was assigned to the transitions from S_0 to S_2 and S_0 to S_3. The transition of S_0 to S_1 is symmetrically forbidden, akin to other symmetric CPPs.[19]

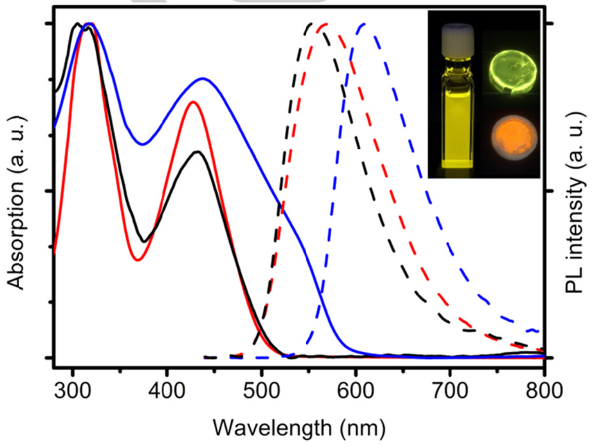

Figure 3. Optical properties of TB[12]CPP. (a) absorption (solid lines) and PL spectra (dashed lines) of TB[12]CPP in chloroform solution (red), powder (blue) and PMMA film (black). Photographs of the solution, powder and PMMA film TB[12]CPP under a UV lamp are shown as the insert figure.

The PL spectrum of TB[12]CPP in chloroform shows a emission peak at 569 nm, which is attributed to the transition of S_1 to S_0 by TD-DFT calculations (Figure S11). Owing to the symmetry broken in the excited state, the forbidden transition of S_0 to S_1 in the ground state becomes allowed in the excited state, accounting for the large Stokes-shift (142 nm) of TB[12]CPP. Compared with emission of [12]CPP at 450 nm and 4,7-diphenyl-benzothiadiazole at 501 nm (Figure S6), the emission of TB[12]CPP is red-shifted by 119 nm and 68 nm in chloroform. The PLQY of TB[12]CPP in chloroform were measured to be 81% in terms of the absolute method using integrating sphere, higher than that of 4,7-diphenyl-benzothiadiazole (61%) and the reported CPPs with emission in the similar wavelength range.[8-9] The PL of TB[12]CPP in different solvents was investigated. As shown Table S1, with increasing polarity of solvents, the PL peaks shift from 555 nm to 586 nm, corresponding to a color change of PL from lime to orange (Figure S7). The linear relationship between the wavenumber of TB[12]CPP emission in different solvent and the solvent parameter $ET_{(30)}$ (Figure S8) [20] manifests a positive solvatofluorochromism of TB[12]CPP. The PLQY measured in these solvent ranges from 82% to 59% (Table S1), demonstrating a good solvent tolerance.

In addition, the UV-Vis absorption and PL of TB[12]CPP in solid state were further investigated. The TB[12]CPP powder showed two broadened absorption bands at 317 and 440 nm and an absorption onset shifted to 600 nm (Figure 3). Similarly, the PL of TB[12]CPP powder red-shifted to 610 nm. Such red-shift observed implies strong intermolecular interactions in the powder. Consequentially, it is not surprising that the PLQY of TB[12]CPP powder decreased to 12%, caused by aggregation-induced quenching. In contrast, in polymethyl methacrylate (PMMA) film, the profile of absorption and PL spectra of TB[12]CPP keeps nearly unchanged (Figure 3), indicating a well dispersion of TB[12]CPP in PMMA matrix. Interestingly, the PLQY in PMMA film increases to 98%, owing to the reduced molecular collision of TB[12]CPP in the solid matrix. The bright emission of TB[12]CPP in solid matrix promises its applications in organic optical devices.

The cyclic structure of CPPs is suitable for supramolecular assembly. The supramolecular complexes of CPPs and fullerenes were most widely investigated, which could mimic the CNT peapods[10a, 10b]. As revealed by SCXRD, the inner cavity of TB[12]CPP has an average diameter of 16.5 Å, much larger than C_{60}. Instead, fullerene derivatives have larger molecular size and its functional group can afford additional intermolecular interactions with CPPs. Accordingly, we chose anthracene-C_{60} as the guest molecule to assemble with TB[12]CPP. By evaporating the carbon disulfide solution of anthracene-C_{60} and TB[12]CPP, their cocrystals can be obtained. As shown in Figures 4a and 4b, anthracene-C_{60} assembles into the inner cavity of TB[12]CPP in a “slant standing” orientation. The binding constant (K_a) of anthracene-C_{60}@TB[12]CPP in toluene was measured to be $1.87 \pm 0.05 \times 10^4$ M^{-1} by fluorescence titration (Supporting Information S5 and Figure S13). As a result of accommodation of elongated anthracene-C_{60}, the hoop of TB[12]CPP was deformed into an elliptical comformation with long and short axis of 17.8 and 14.7 Å, respectively (Figure 4h). Of interest, anthracene-C_{60} interacts with the π-system of TB[12]CPP by π–π interactions (3.25-3.42 Å, pink dash lines in Figure 4a) of fullerene cage and C-H$\cdots\pi$ interactions[21] (2.7 Å) of anthracene moiety, which exemplifies the first case of CPP complex combining with π–π and C-H$\cdots\pi$ interactions.

The supramolecular structures of $(DMF)_4$@TB[12]CPP suggests the possibility to host a supramolecular complex in the hoop of TB[12]CPP. Then we screened a series of ternary cocrystallization of TB[12]CPP, fullerene and small PAHs, and finally the ternary cocrystals of TB[12]CPP, C_{60}/C_{70} and trithiasumanene[22] were obtained by solvent evaporation. Shown in SCXRD structures (Figures 4c-4f), inside the ring of TB[12]CPP, C_{60}/C_{70} and trithiasumanene assemble in a concave-convex manner with the shortest intermolecular C$\cdots$C distance of 3.15 Å, implying their strong π–π interactions. Trithiasumanene$\supset C_{60}$/C_{70} complex adopts a “slant standing” orientation related to TB[12]CPP as well (Figures 4d and 4f). Between trithiasumanene$\supset C_{60}$/C_{70} and TB[12]CPP, the fullerene end of inner complex interacts with TB[12]CPP by π–π interactions with the C$\cdots$C distances range from 3.31 to 3.42 Å (Figures 4c and 4e), while hydrogens of trithiasumanene forms C-H$\cdots\pi$ interactions with the phenylene unit of TB[12]CPP (Figures 4c and 4e), which manifests the formation of ternary complex (trithiasumanene$\supset C_{60}$/C_{70})@TB[12]CPP. Different from the circular comformation in $(DMF)_4$@TB[12]CPP and elliptical comformation in anthracene-C_{60}@TB[12]CPP and (trithiasumanene$\supset C_{60}$)@TB[12]CPP, an oval shaped TB[12]CPP was observed in (trithiasumanene$\supset C_{70}$)@TB[12]CPP (Figures 4g-4j), propably due to the larger size of C_{70}, which establishes TB[12]CPP as a shape-adaptable host.

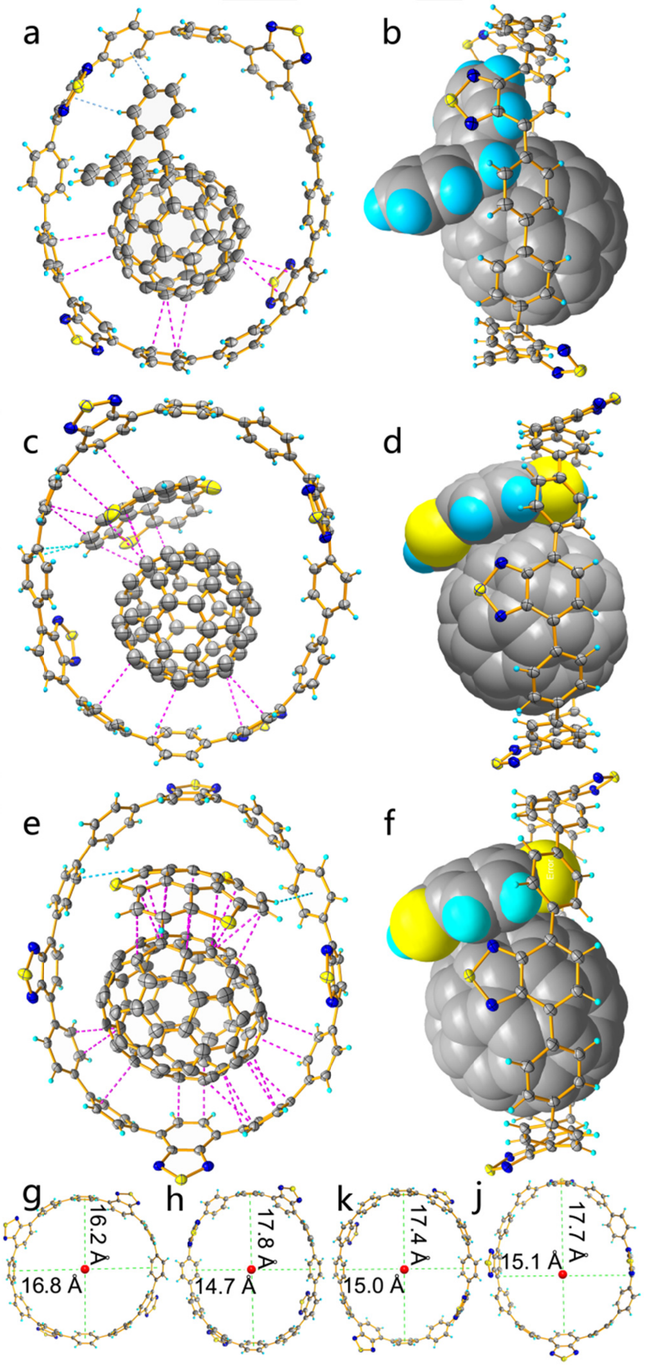

Figure 4. Structures of the supramolecular assembly of TB[12]CPP. (a. b.) top and side views of anthracene-C_{60}@TB[12]CPP. (c. d.) top and side views of (trithiasumanene$\supset C_{60}$)@TB[12]CPP. (e. f.) top and side views of

(trithiasumanene$\supset C_{70}$)@TB[12]CPP. The $\pi-\pi$ and C-H$\cdots\pi$ interactions are represented by pink and sky blue dash lines, respectively. The inner guests in the side views were represented in spacefill model for clarity. The structures of TB[12]CPP in $(DMF)_4$@TB[12]CPP (g), anthracene-C_{60}@TB[12]CPP (h), (trithiasumanene$\supset C_{60}$)@TB[12]CPP (j) and (trithiasumanene$\supset C_{70}$)@TB[12]CPP (k). The centroids of hoop were represented by the red dots. The shortest and longest distances through the centroid were shown as green dash lines.

The binding constants of (trithiasumanene$\supset C_{60}$)@TB[12]CPP and (trithiasumanene$\supset C_{70}$)@TB[12]CPP in toluene were determined to be 2.14±0.10 × 10^4 M^{-1} and 4.80±0.07 × 10^4 M^{-1}, respectively, by fluorescence titration (Supporting Information S5 and Figure S13). In comparison with dynamic binding of C_{60} (K_{sv} = 1.60±0.03 × 10^4 M^{-1}) and smaller binding constant of C_{70} to TB[12]CPP (K_a = 3.20±0.07 × 10^4 M^{-1}) (Figures S12 and S13), a cooperative binding effects of trithiasumanene$\supset C_{60}/C_{70}$ was suggested. As expected, DFT calculations of these TB[12]CPP complexes clearly reveal the larger binding affinities for (trithiasumanene$\supset C_{60}/C_{70}$)@TB[12]CPP (-60.94 and -66.37 Kcal M^{-1}), compared with that of C_{60}/C_{70}@TB[12]CPP (-36.44 and -42.55 Kcal M^{-1}) (Figure S14).

In summary, a highly emissive TB[12]CPP was synthesized by introducing four benzothiadiazole units into the carbon backbone. Different from blue emission of the reported bright CPP, a lime to orange emission of TB[12]CPP with high PLQY (82% to 59%) was achieved in different solvents. The PLQY of TB[12]CPP in polymer matrix can further increase to 98%. These enhanced optical properties can promise its applications in fluoresce imaging and optical organic devices. Benefiting from the enlarged inner space, TB[12]CPP assemble with anthracene-C_{60} or trithiasumanene$\supset C_{60}/C_{70}$ complex by both $\pi-\pi$ and C-H$\cdots\pi$ interactions. The latter one realizes the ternary assembly of CPP. These assemblies of TB[12]CPP establishes the ability of large CPPs to accommodate complex guests and suggests the possibility to create the CNT peapods filled with supramolecular complex.

Acknowledgements

This work was financially supported by the Ministry of Science and Technology of China (2017YFA0204902, 2018YFA0209500) and the National Natural Science Foundation of China (21771155, 21721001). The authors thank Prof. Xu Hou for beneficial discussion.

Keywords: cycloparaphenylene, photo luminescence, fluorophore, supramolecular assembly

---

[1] S. E. Lewis, *Chem. Soc. Rev.* **2015**, *44*, 2221-2304.
[2] H. Omachi, T. Nakayama, E. Takahashi, Y. Segawa, K. Itami, *Nat. Chem.* **2013**, *5*, 572-576.
[3] a) W. S. Rapson, R. G. Shuttleworth, J. N. van Niekerk, *J. Chem. Soc.* **1943**, 326-327; b) H. A. Staab, F. Binnig, *Tetrahedron Lett.* **1964**, *5*, 319-321.
[4] a) R. Jasti, J. Bhattacharjee, J. B. Neaton, C. R. Bertozzi, *J. Am. Chem. Soc.* **2008**, *130*, 17646-17647; b) H. Takaba, H. Omachi, Y. Yamamoto, J. Bouffard, K. Itami, *Angew. Chem. Int. Ed.* **2009**, *48*, 6112-6116.
[5] E. J. Leonhardt, R. Jasti, *Nat. Rev. Chem.* **2019**, *3*, 672-686.
[6] E. R. Darzi, R. Jasti, *Chem. Soc. Rev.* **2015**, *44*, 6401-6410.
[7] a) H. Tang, Z. Gu, C. Li, Z. Li, W. Wu, X. Jiang, *Biomater. Sci.* **2019**, *7*, 2552-2558; b) B. M. White, Y. Zhao, T. E. Kawashima, B. P. Branchaud, M. D. Pluth, R. Jasti, *ACS Cent. Sci.* **2018**, *4*, 1173-1178.
[8] a) S. Yamago, Y. Watanabe, T. Iwamoto, *Angew. Chem. Int. Ed.* **2010**, *49*, 757-759; b) T. J. Sisto, M. R. Golder, E. S. Hirst, R. Jasti, *J. Am. Chem. Soc.* **2011**, *133*, 15800-15802.
[9] a) E. R. Darzi, E. S. Hirst, C. D. Weber, L. N. Zakharov, M. C. Lonergan, R. Jasti, *ACS Cent. Sci.* **2015**, *1*, 335-342; b) T. Kuwabara, J. Orii, Y. Segawa, K. Itami, *Angew. Chem. Int. Ed.* **2015**, *54*, 9646-9649.
[10] a) Y. Xu, M. von Delius, *Angew. Chem. Int. Ed.* **2020**, *59*, 559-573; b) D. Lu, Q. Huang, S. Wang, J. Wang, P. Huang, P. Du, *Front. Chem.* **2019**, *7*; c) M. B. Minameyer, Y. Xu, S. Frühwald, A. Görling, M. von Delius, T. Drewello, *Chem. Eur. J.* **2020**, *doi:10.1002/chem.202001503*.
[11] a) T. Iwamoto, Y. Watanabe, T. Sadahiro, T. Haino, S. Yamago, *Angew. Chem. Int. Ed.* **2011**, *50*, 8342-8344; b) T. Iwamoto, Y. Watanabe, H. Takaya, T. Haino, N. Yasuda, S. Yamago, *Chem. Eur. J.* **2013**, *19*, 14061-14068.
[12] a) T. Matsuno, K. Fukunaga, S. Sato, H. Isobe, *Angew. Chem. Int. Ed.* **2019**, *58*, 12170-12174; b) T. Matsuno, M. Fujita, K. Fukunaga, S. Sato, H. Isobe, *Nat. Commun.* **2018**, *9*, 3779.
[13] D. Lu, G. Zhuang, H. Wu, S. Wang, S. Yang, P. Du, *Angew. Chem. Int. Ed.* **2017**, *56*, 158-162.
[14] Y. Wang, T. Michinobu, *J Mater. Chem. C* **2016**, *4*, 6200-6214.
[15] T. C. Lovell, Z. R. Garrison, R. Jasti, *Angew. Chem. Int. Ed.* **2020**, *doi:10.1002/anie.202006350*.
[16] I. Alkorta, I. Rozas, J. Elguero, *Chem. Soc. Rev.* **1998**, *27*, 163-170.
[17] Y. Segawa, S. Miyamoto, H. Omachi, S. Matsuura, P. Šenel, T. Sasamori, N. Tokitoh, K. Itami, *Angew. Chem. Int. Ed.* **2011**, *50*, 3244-3248.
[18] E. R. Darzi, T. J. Sisto, R. Jasti, *J. Org. Chem.* **2012**, *77*, 6624-6628.
[19] T. C. Lovell, C. E. Colwell, Lev N. Zakharov, R. Jasti, *Chem. Sci.* **2019**, *10*, 3786-3790.
[20] C. Reichardt, *Chem. Rev.* **1994**, *94*, 2319-2358.
[21] M. Nishio, *Phys. Chem. Chem. Phys.* **2011**, *13*, 13873-13900.
[22] Q. Tan, D. Zhou, T. Zhang, B. Liu, B. Xu, *Chem. Commun.* **2017**, *53*, 10279-10282.

COMMUNICATION

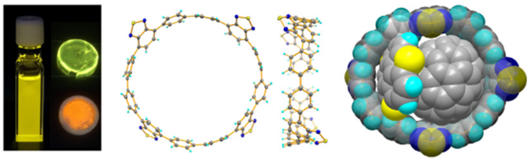

Bright host : A benzothiadiazole-based [12]cycloparaphenylene (TB[12]CPP) is obtained and characterized. TB[12]CPP exhibits a lime to orange emission with a quantum yield up to 98%, ranking it as one of brightest CPPs. As a supramolecular host, TB[12]CPP is “bright” as well, showing adaptable ring structure. A ternary assembly between TB[12]CPP, fullerene and buckybowl is realized.

Z. L. Qiu, C. Tang, X. R. Wang, Y. Y. Ju, K. S. Chu, Z. Y. Deng, H. Hou, Dr. Y.M. Liu, Prof. Dr. Y. Z. Tan

Page No. – Page No.

Tetra-benzothiadiazole-based [12]Cycloparaphenylene with Bright Emission and its Supramolecular Assembly